3D Percolation Theory-Based Exposure-Path Prevention for Optimal Power-Coverage Tradeoff in Clustered Wireless Camera Sensor Networks

Jingqing Wang† and Xi Zhang†‡

†Networking and Information Systems Laboratory
Dept. of Electrical and Computer Engineering, Texas A&M University, College Station, TX 77843, USA
‡National Mobile Communications Research Laboratory, Southeast University, Nanjing, P. R. China
E-mail: {*wang12078@neo.tamu.edu*, *xizhang@ece.tamu.edu*}

***Abstract*—With fast advances in camera sensor devices and wide applications of wireless camera sensor networks (WCSNs), optimizing the tradeoff between power consumption and coverage rate of WCSNs attracts a great deal of research attention. In contrast to 2D WCSNs, 3D WCSNs capture more accurate and comprehensive information for surveillant applications. The percolation theory has been proved to be powerful and effective in characterizing the exposure path prevention using 2D WCSNs. While percolation theory can be potentially extended into 3D WCSNs to improve the power and coverage performances, there are still many new challenges remaining unsolved. On the other hand, the clustering algorithm is widely cited as an efficient power saving and interference mitigation technique for WCSNs. However, how to integrate the clustering technique with 3D percolation theory in WCSNs is still an open problem. To overcome the aforementioned challenges, in this paper we propose the 3D percolation theory-based exposure-path prevention scheme for optimizing the tradeoff between power consumption and coverage rate over clustered WCSNs. First, we apply and extend the bond-percolation theory to derive the optimal density of camera sensors deployed in 3D WCSNs subject to the minimum exposure-path prevention probability constraint. Then, we apply the mutual entropy to analyze the dependency among 3D neighboring camera sensors, justifying the bond-percolation theory in 3D WCSNs. Finally, we apply the new low energy adaptive clustering hierarchy (LEACH) architecture into our 3D WCSNs for power saving and interference mitigation. The conducted extensive simulations show that our proposed schemes outperform the other existing schemes in optimizing the tradeoff between power consumption and coverage rate over 3D WCSNs.**

***Index Terms*—3D WCSNs, exposure-path prevention, percolation theory, NEW LEACH, optimal power-coverage tradeoff**

I. Introduction

THE rapid development in VLSI device and image sensor techniques has enabled the cost-effective development of the large-scale, small-size, and energy-saving wireless camera sensor networks (WCSNs). As a result, how to efficiently design and implement WCSNs in many critical applications, such as the battlefield surveillance, homeland security, industrial process supervision, and health monitoring systems has received a great deal of research attention from both academia and industry [1].

One of the key issues in designing and implementing WCSNs is how to optimize the tradeoff between power consumption and coverage rate. Most existing works on sensor coverage mainly focus on full coverage models. In contrast, many applications focus on the exposure-path prevention, which only needs partial coverage. The percolation theory has been proved to be powerful and effective in solving the exposure-path prevention problem in 2D WCSNs. While percolation theory can be also potentially extended into 3D models to future improve the power and exposure-path prevention performance, there are still many new challenges remaining unsolved.

On the other hand, the clustering algorithm is widely cited as an efficient power saving and interference mitigation technique for 2D WCSNs. There are many existing works on the clustering algorithm [2] [3]. However, how to integrate the clustering technique with 3D percolation theory for optimizing the power-saving subject to the minimum coverage rate constraint in 3D WCSNs still remains as an open problem.

To overcome the above-mentioned challenges, we propose the 3D percolation theory-based exposure-path prevention scheme for optimizing the tradeoff between power consumption and coverage rate over clustered WCSNs. First, we formulate and solve the exposure-path prevention problem under the percolation theory [4], [5]. We derive the critical density of camera sensors subject to the minimum exposure-path prevention probability constraint using bond-percolation theory. We also model and analyze the mutual dependency among 3D neighboring camera sensors, justifying the feasibility of application of the bond-percolation theory in 3D WCSNs. Finally, using the critical sensor density derived, we can develop the NEW-LEACH-based scheme to derive the optimal probability of selecting cluster heads, minimizing power consumption and interference.

The rest of this paper is organized as follows: Section II establishes the FOV model for 3D WCSNs and the bond-percolation model. Section III formulates the coverage problem to derive the optimal density for exposure path and mea-

This work was supported in part by the U.S. National Science Foundation under Grant CNS-1205726, the U.S. National Science Foundation CAREER Award under Grant ECCS-0348694, the Open Research Fund of National Mobile Communications Research Laboratory, Southeast University (No. 2012D12).

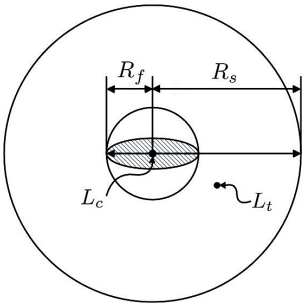

Fig. 1. 3D omnidirectional model for WCSNs.

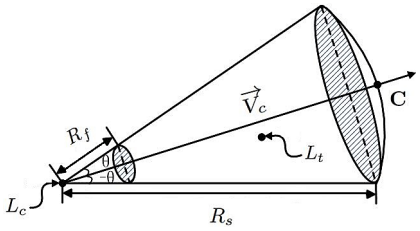

Fig. 2. 3D directional model for WCSNs.

sures the mutual dependency among 3D neighboring camera sensors. Section IV uses the NEW-LEACH to determine the threshold for cluster head selection. Section V validates and evaluates our proposed schemes by simulations. The paper concludes with Section VI.

II. The System Model

There are two types of 3D sensing models: the omnidirectional model and directional model, shown in Fig. 1 and Fig. 2, respectively. Our system models are under the following assumptions: (1) All camera sensors have the same sensing radius. For directional sensing model, all sensors also have the same sensing angle 2θ, and the same field of view (FOV) as shown in Fig. 2; (2) All sensors transmit at the same power level; (3) Each camera sensor uses 1 unit of energy to transmit or receive 1 unit of data.

A. 3D Sensing Model

The 3D omnidirectional model is based on the sphere model for omnidirectional WCSNs. Let $L_c(x_c, y_c, z_c)$ denote the location of the camera sensor. R_s denotes the sensing radius. As shown in Fig. 1, the omnidirectional model for a camera sensor is a 3D sphere space centered at L_c. A target point $L_t(x_t, y_t, z_t)$ in the 3D space is said to be covered if

$$|L_c L_t| \leq R_s \tag{1}$$

where the Euclidean distance between $|L_c L_t|$ is

$$d_{ct} = \sqrt{(x_t - x_c)^2 + (y_t - y_c)^2 + (z_t - z_c)^2}. \tag{2}$$

In addition, the radius of the blind area is denoted as R_f. If the distance between the target and the sensor node is less than R_f, the target cannot be detected. From the omnidirectional model, we can derive the sensing volume V_o as follows,

$$V_o = \frac{4\pi \left(R_s^3 - R_f^3\right)}{3}. \tag{3}$$

The 3D directional model is based on the FOV in WCSNs. As shown in Fig. 2, FOV for directional sensing model is defined as a cone with 4 tuples $\left(L_c, R_s, \overrightarrow{V_c}, \theta\right)$, where $L_c(x_c, y_c, z_c)$ is the location of the camera sensor; R_s is the sensing radius; $\overrightarrow{V_c}$ is the sensing direction; $\{-\theta, \theta\}$ is the offset angle on both sides of $\overrightarrow{V_c}$. In addition, the radius of the blind area is denoted as R_f. A target is said to be covered if and only if the following conditions hold:

1) $|L_c L_t| = d_{ct} \leq R_s$;
2) the offset angle between $\overrightarrow{L_c L_t}$ and $\overrightarrow{V_c}$ is within $[0, \theta]$.

where d_{st} is spesified by Eq. (2).

We can derive the directional sensing volume, denoted by V_d, as follows,

$$V_d = \frac{2\pi \left(R_s^3 - R_f^3\right)(1 - \cos(\theta))}{3}. \tag{4}$$

B. 3D Sensor Deployment Model

The sensors are distributed as a stationary Poisson process. The location of each sensor is identically and independently distributed (i.i.d.). Let k be a positive integer, N denote the number of camera sensors deployed in the 3D sensing space V. The probability that there are k sensors in V is given by

$$\Pr\{N = k\} = \frac{(\lambda \|V\|)^k}{k!} e^{-\lambda \|V\|} \tag{5}$$

where $\|V\|$ is the total volume of the 3D sensing space V. The offset angle θ is uniformly distributed over $[0, \pi]$.

C. The Bond-Percolation Model For Exposure-Path Prevention

As defined in [1], a continuous curve from one side of the deployment space to the opposite side is said to be an exposure path if the continuous curve belongs to a 3D vacant space which is not covered by any sensing sphere. According to percolation theory, we can define the critical density of camera sensors, denoted by λ_c. If $\lambda \leq \lambda_c$, there exists exposure paths in the sensor-deployed space a.s. We model the exposure-path problem by a 3D lattice with the length $2a$ of each side, see Fig. 3. The lattice contains M^3 vertexes with M vertexes along each side of the lattice, denoted by $V_e = \{v_1, v_2, ..., v_{M^3}\}$. Let $e_{i,j}$ denote the edge between two vertexes v_i and v_j, where $i, j \in [1, 2, ..., M^3]$. Any two vertexes connected by a common edge are called the neighboring vertexes. We use two definitions to characterize whether edge $e_{i,j}$ is open or closed, which can yield the lower bound and upper bound of the critical density for 3D WCSNs.

Definition 1: *L-closed/L-open Edge*. If at least one point on the edge $e_{i,j}$ is covered by a sensor network, then $e_{i,j}$ is said to be an *L-closed* edge. Otherwise, $e_{i,j}$ is called *L-open*.

Definition 2: *U-closed/U-open Edge*. If all points on the edge $e_{i,j}$ are covered by one camera sensor network, then $e_{i,j}$ is called as *U-closed*. Otherwise, $e_{i,j}$ is called *U-open*.

Define two functions to determine whether $e_{i,j}$ is closed or not. For *L-closed/L-open* edges, $L(e_{i,j}) = 1$, if at least one point on $e_{i,j}$ is covered; Otherwise, $L(e_{i,j}) = 0$. For *U-closed/U-open* edges, $U(e_{i,j}) = 1$, if all points on $e_{i,j}$ are

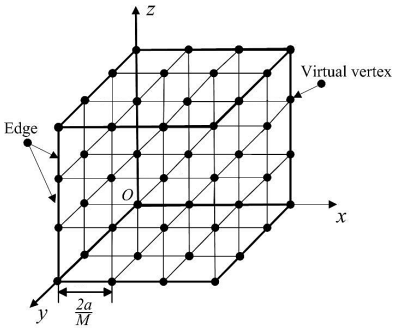

Fig. 3. 3D lattice for WCSNs.

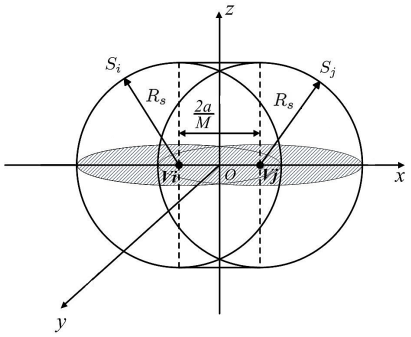

Fig. 4. The covered volume for edge $e_{i,j}$.

covered; Otherwise, $U(e_{i,j}) = 0$. Then, derive the following two probabilities for *L-closed* edges and *U-closed* edges:

$$\begin{cases} p_l \triangleq \Pr\{L(e_{i,j}) = 1\}, \\ p_u \triangleq \Pr\{U(e_{i,j}) = 1\}. \end{cases} \tag{6}$$

Therefore, we can use L-coverage lattice to derive the lower bound of the critical density of camera sensors, and U-coverage lattice to derive the upper bound for the critical density of camera sensors.

III. The Critical Density of Camera Sensors

We assume that the probability whether all edges are closed or not is independent under bond-percolation theory. However, $p_l(p_u)$ of edge $e_{i,j}$ depends on $p'_l s(p'_u s)$ of the neighboring edges in reality. We will analyze the dependency issues in Section III-C. Define p_c to be the percolation threshold. For all $p > p_c$, there exists one closed path extending from one side to another, whereas for all $p < p_c$, there exists no exposure path. As proved in [6], percolation threshold p_c for 3D lattice is equal to 0.2488. Therefore, if $p_l < 0.2488$, there exists exposure paths; if $p_u > 0.2488$, there is no exposure path. The deployed camera sensor density denoted by λ_l for L-coverage lattice and λ_u for U-coverage lattice are as follows,

$$\begin{cases} \lambda_l \triangleq \sup\{\lambda \mid p_l \le 0.2488\}, \\ \lambda_u \triangleq \inf\{\lambda \mid p_u \ge 0.2488\}. \end{cases} \tag{7}$$

Then, define the critical density, denoted by λ_c, of camera sensors, satisfying the following inequations $\lambda_l < \lambda_c < \lambda_u$.

A. Critical Camera Sensor Density for Omnidirectional Model

Let t_n be any point on edge $e_{i,j}$. Define $S_i \bigsqcup S_j$ as follows:

$$S_i \bigsqcup S_j \triangleq \bigcup_{\forall t_n \in e_{i,j}} S_n \tag{8}$$

where S_n is the sphere centered around t_n with radius R_s, as shown in Fig. 4; S_i is the sphere centered at V_i and S_j is the sphere centered at V_j. Assuming that all points on edge $e_{i,j}$ are not covered if and only if there is no sensor node within the space $S_i \bigsqcup S_j$, we derive the following equations [1]:

$$\begin{cases} \lambda_l = -\frac{\log(1-p_l)}{V_1}, \\ \lambda_u < -\frac{\log(1-p_u)}{V_2} \end{cases} \tag{9}$$

where

$$\begin{cases} V_1 = \frac{4}{3}\pi R_s^3 + 2\pi\frac{aR_s^2}{M}, \\ V_2 = 8\int_{S_i \bigcap S_j} d\vec{\boldsymbol{v}} \end{cases} \tag{10}$$

where we define $d\vec{\boldsymbol{v}} \triangleq dxdydz$; V_1 is the volume of $S_i \bigsqcup S_j$ and V_2 is the volume of $S_i \bigcap S_j$. Thus, we can derive the lower and upper bound for critical density, denoted by λ_c^o of omnidirectional camera sensors in as follows:

$$\frac{-\log(1-p_l)}{\frac{4}{3}\pi R_s^2 + \frac{4aR_s}{M}} < \lambda_c^o < \frac{-\log(1-p_u)}{V_1}. \tag{11}$$

B. The Critical Camera Sensor Density for Directional Model

Suppose there is a directional camera sensor at point $L_c(x, y, z)$ in $S_i \bigsqcup S_j$. A sphere centered at L_c with radius R_s intersects x-axis at point $D_1(x - \sqrt{R_s^2 - y^2 - z^2}, 0, 0)$ and $D_2(x + \sqrt{R_s^2 - y^2 - z^2}, 0, 0)$. Let $d_1 = x - \sqrt{R_s^2 - y^2 - z^2}$ and $d_2 = x + \sqrt{R_s^2 - y^2 - z^2}$. Define $\langle \vec{a}, \vec{b} \rangle$ to be the angle between $\vec{a}$ and $\vec{b}$. Then if $e_{i,j}$ is *L-closed*, we can derive the following equations [1]:

$$\lambda_l = \frac{-\log(1-p_l)}{\int_{S_i \bigsqcup S_j} \left(1 - p_n^{(1)}\right) d\vec{\boldsymbol{v}}} \tag{12}$$

where we can further derive the probability that a directional camera sensor in $S_i \bigsqcup S_j$ cannot cover any point on $e_{i,j}$, denoted by $p_n^{(1)}$, as follows:

$$p_n^{(1)} = \begin{cases} \frac{2\pi - 2\theta - \langle \overrightarrow{L_c v_i}, \overrightarrow{L_c D_2} \rangle}{2\pi}, & \text{if } d_1 < -\frac{a}{m} \text{ and } |d_2| < \frac{a}{M}; \\ \frac{2\pi - 2\theta - \langle \overrightarrow{L_c D_1}, \overrightarrow{L_c D_2} \rangle}{2\pi}, & \text{if } -\frac{a}{m} < d_1 < d_2 < \frac{a}{M}; \\ \frac{2\pi - 2\theta - \langle \overrightarrow{L_c v_i}, \overrightarrow{L_c v_j} \rangle}{2\pi}, & \text{if } d_1 < -\frac{a}{m} \text{ and } d_2 > \frac{a}{M}; \\ \frac{2\pi - 2\theta - \langle \overrightarrow{L_c D_1}, \overrightarrow{L_c v_j} \rangle}{2\pi}, & \text{if } |d_1| < \frac{a}{m} \text{ and } d_2 > \frac{a}{M}. \end{cases} \tag{13}$$

Then, if $e_{i,j}$ is an arbitrary edge in U-coverage lattice in directional WCSNs, we have the following equations [1],

$$p_u > 1 - \exp\left(-\lambda_u \int_{S_i \bigcap S_j} \left(1 - p_n^{(2)}\right) d\vec{\boldsymbol{v}}\right) \tag{14}$$

where the probability $p_n^{(2)}$ that the directional sensor in $S_i \bigcap S_j$ cannot cover any point on $e_{i,j}$ is derived as follows:

$$p_n^{(2)} = \begin{cases} 1, & \text{if } \langle \overrightarrow{L_c v_i}, \overrightarrow{L_c v_j} \rangle > 2\theta; \\ \frac{2\pi - 2\theta - \langle \overrightarrow{L_c v_i}, \overrightarrow{L_c v_j} \rangle}{2\pi}, & \text{otherwise.} \end{cases} \tag{15}$$

Thus, we can derive the lower and upper bound for critical density, denoted by λ_c^d, of camera sensors as follows:

$$\frac{-\log(1-p_l)}{\int_{S_i \bigsqcup S_j}\left(1-p_n^{(1)}\right)d\vec{\boldsymbol{v}}} < \lambda_c^d < \frac{-\log(1-p_u)}{\int_{S_i \bigcap S_j}\left(1-p_n^{(2)}\right)d\vec{\boldsymbol{v}}}. \tag{16}$$

C. Dependence Among Neighboring Edges

In reality, $p_l(p_u)$ of edge $e_{i,j}$ is not independent of $p_l's(p_u's)$ of its neighboring edges. However, in bond-percolation theory, whether all edges are closed or not is independent. Thus, we also need to model and analyze the dependency among neighboring edges. In our 3D model, without loss of generality, we consider edge $e_{1,2}$'s dependency on its neighboring edges. In particular, edge $e_{1,2}$ has 5 neighboring edges $e_{1,3}$, $e_{1,4}$, $e_{1,5}$, $e_{1,6}$ and $e_{1,7}$. According to [7] and [8], we define *n*-variable mutual entropy which quantifies the amount of mutual information that is shared among n random variables. The n-variable mutual entropy is defined as follows:

$$\begin{aligned} &I(X_1, X_2, ..., X_n) \\ =&\sum_{x_1\in\varphi, x_2\in\varphi, ..., x_n\in\varphi} P_{\mathbf{X}}(x_1, x_2, ..., x_n)\log\frac{P_{\mathbf{X}}(x_1, x_2, ..., x_n)}{\prod_{i=1}^{n} P_{X_i}(x_i)} \end{aligned} \tag{17}$$

where n-variable random vector $\mathbf{X} = (X_1, X_2, ..., X_n)$; $\varphi = \{0, 1\}$; $P_{\mathbf{X}}(x_1, x_2, ..., x_n)$ is the joint probability mass function (PMF) of $X_1, X_1, ..., X_n$ and $P_{X_i}(x_i)$ is the marginal PMF of x_i, for $i = 1, 2, ..., n$.

For L-coverage lattice with $n = 6$, see Fig. 3. we define

$$\begin{cases} P_{\mathbf{X}}(x_1, ..., x_6) = \Pr\{L(e_{1,2}) = x_1, ..., L(e_{1,7}) = x_6\}, \\ P_{X_1}(x_1) = \Pr\{L(e_{1,2}) = x_1\}, \\ ... \\ P_{X_6}(x_6) = \Pr\{L(e_{6,7}) = x_6\} \end{cases} \tag{18}$$

where $x_1, ..., x_6 \in \varphi$.

As for *n*-variable mutual entropy $I(U(e_{1,2}), ..., U(e_{1,7}))$ for U-coverage lattice, the definition is similar, but we use $P_{\mathbf{Y}}(y_1, ..., y_6)$ and $P_{Y_i}(y_i)$ instead, where $\mathbf{Y} = (Y_1, Y_2, Y_3, Y_4, Y_5, Y_6)$ and $y_1, ..., y_6 \in \varphi$.

We can calculate $I(X_1, X_2, ..., X_6)$ for our omnidirectional model. From Eq. (10), for $i = 1, ..., 6$, we have

$$\begin{cases} P_{X_i}(0) = e^{-\lambda V_1}, \\ P_{X_i}(1) = 1 - e^{-\lambda V_1}. \end{cases} \tag{19}$$

where the value of V_1 is determined by Eq. (11). Furthermore, we have

$$P_{\mathbf{X}}(0,0,0,0,0,0) = \Pr\left\{N\left(\bigsqcup_{i=1,...,6} S_i = 0\right)\right\}. \tag{20}$$

According to the identity for converting the joint distribution to the product of conditional distribution and marginal distribution, i.e., $P(AB) = P(A|B)P(B)$, we can derive the joint PMF of X_i , where $i = 1, 2, ..., 6$. When $R_s = 10$, $a = 50$, and $n = 100$, we can observe from Fig. 5 that the maximal value for $I(L(e_{1,2}), L(e_{2,3}))$ is about 3.2 and the maximal value for $I(U(e_{1,2}), U(e_{2,3}))$ is about 3.3. Similarly, we can derive $I(X_1, X_2, ..., X_6)$ for directional model. Because of the large-scale feature for 3D WCSNs, there are a large number of camera sensors deployed in the entire sensing space. The mutual dependency among neighboring edges is relatively weak. Therefore, we can approximately apply the bond-percolation theory in our 3D models.

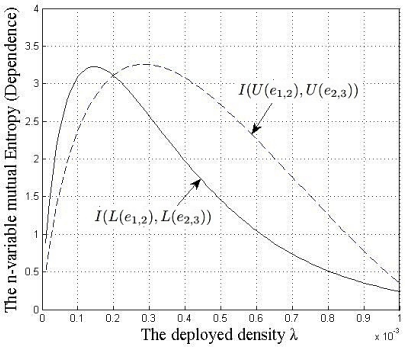

Fig. 5. Analysis and comparison between $I(L(e_{1,2}), ..., L(e_{1,7}))$ and $I(U(e_{1,2}), ..., U(e_{1,7}))$ for omnidirectional WCSNs

IV. New Leach Algorithm

LEACH algorithm has been used to achieve energy efficiency in WCSNs for years. Compared with LEACH, NEW LEACH algorithm considers the different weights among residual energy, energy consumption rate and location information, achieving better performance in saving energy and reducing the interference between camera sensors in WCSNs. However, all previous works directly use a random deployed density λ to derive the threshold for cluster head selection. Under the minimum exposure-path prevention probability constraint, the critical deployed density of camera sensors can be applied in NEW-LEACH algorithm in our paper.

In NEW LEACH algorithm, assuming all nodes are homogeneous, at first all nodes has the same probability to become a cluster head. Let $\xi(g)$ denote the threshold whether node g can be selected as the cluster head. The decision is made at the beginning of each round by each node $g \in G$ independently choosing a random number in $[0, 1]$. If the random number is less than the threshold $\xi(g)$, then node g becomes a cluster head in the current round. The threshold $\xi(g)$ is derived as follows,

$$\xi(g) = \begin{cases} \dfrac{p_\omega W_1 \frac{E_c}{E_0}}{1-p_\omega\left(r \bmod \left(\frac{1}{p_\omega}\right)\right)} + \dfrac{p_\omega W_2 e^{-\frac{E_b - E_c}{E_0}}}{1-p_\omega\left(r \bmod \left(\frac{1}{p_\omega}\right)\right)} \\ + \dfrac{p_\omega W_3\left(\frac{d_a^2}{d_m^2+d_i^2}\right)}{1-p_\omega\left(r \bmod \left(\frac{1}{p_\omega}\right)\right)}, & \text{if } \forall g \in G, \\ 0, & \text{otherwise} \end{cases} \tag{21}$$

where G is the set of non-selected nodes in the previous rounds; r is the current round number per epoch; p_ω is the probability for a sensor to become a cluster head; E_0, E_c, and E_b are the initial energy, current energy and the energy in the former round comparing to the current round

of the sensor node, respectively; d_a and d_m are the average distance and the maximal distance from the sensor nodes to the processing center, respectively; d_i is the distance from the current selected node to the processing center; (W_1, W_2, W_3) is the weight value for the residual energy, energy consumption rate and the location information. As shown in [3], the optimal combination of weights (W_1, W_2, W_3) is $(0.111111, 0.000528, 0.88836)$.

A. Power Saving

We characterize the entire supervisory space as a cube with the side length of $2a$, and the processing center is in the center of the cube. Let Δ_i denotes the length of the segment from sensor i to the processing center. Let $\lambda = \lambda_c^o$ or $\lambda = \lambda_c^d$, which we derived in Section III, we can get

$$\begin{aligned}\mathbb{E}[\Delta_i | N = n] &= \int_V \sqrt{x^2 + y^2 + z^2} \left(\frac{1}{8a^3}\right) d\vec{\boldsymbol{v}} \\ &= 0.961a \end{aligned} \tag{22}$$

where (x, y, z) is the location of the sensor node.

The total power $\mathcal{P}$ used by the sensors to communicate 1 unit of data to the cluster head is

$$\begin{aligned}\mathbb{E}[\mathcal{P}] &= \mathbb{E}[\mathbb{E}[\mathcal{P}|N = n]] \\ &= \mathbb{E}[N] \left(\frac{1 - p_\omega}{2R_c\sqrt{p_\omega \lambda}} + \frac{0.961 p_\omega a}{R_c}\right) \\ &= \lambda \|V\| \left(\frac{1 - p_\omega}{2R_c\sqrt{p_\omega \lambda}} + \frac{0.961 p_\omega a}{R_c}\right). \end{aligned} \tag{23}$$

where R_c is the radio distance of the sensor node. Then, taking the first derivative over Eq. (24) yields

$$\frac{\partial \mathbb{E}[\mathcal{P}]}{\partial p_\omega} = -\frac{\sqrt{\lambda}\|V\|}{4R_c\sqrt{p_\omega}} - \frac{\sqrt{\lambda}\|V\|}{4R_c p_\omega^{\frac{3}{2}}} + \frac{0.961\lambda\|V\|a}{R_c}. \tag{24}$$

The second derivative over Eq. (23) yields

$$\frac{\partial^2 \mathbb{E}[\mathcal{P}]}{\partial p_\omega^2} = \frac{\sqrt{\lambda}\|V\|}{8R_c p_\omega^{\frac{3}{2}}} + \frac{3\sqrt{\lambda}\|V\|}{8R_c p_\omega^{\frac{5}{2}}} > 0. \tag{25}$$

Thus, the only real valued root p_ω^* for Eq. (24) is

$$\begin{aligned} p_\omega^* = \Bigg\{ &\frac{1}{11.532a\sqrt{\lambda}} \\ &+ \frac{0.109}{a\sqrt{\lambda}\sqrt[3]{2 + 398.961a^2\lambda + 11.532\sqrt{3\lambda(398.961a^2\lambda + 4)}}} \\ &+ \frac{\sqrt[3]{2 + 398.961a^2\lambda + 11.532\sqrt{3\lambda(398.961a^2\lambda + 4)}}}{11.532a\sqrt{\lambda}\sqrt[3]{2}} \Bigg\}^2. \end{aligned} \tag{26}$$

which will be used in Eq. (21) by setting $p_\omega = p_\omega^*$.

B. Mitigation of Interference

NEW-LEACH algorithm can also mitigate the interference among massive sensor nodes, which is measured by the signal-to-interference-plus-noise ratio (SINR) [9] [10]. We define $\text{SINR}_{i,j}$ between node i and node j as follows:

$$\text{SINR}_{i,j} = \frac{P_T \mathcal{L}(d_{i,j})}{\sigma^2 + \gamma \sum_{k \neq i,j} P_T \mathcal{L}(d_{i,j})} \tag{27}$$

where P_T is the transmit power; σ^2 is the power of the background thermal noise; γ is the inverse of the processing gain of the system, depending on the technology applied in the system, $\gamma \leqslant 1$; $\mathcal{L}(d_{i,j})$ is the path-loss function for wireless channel, where $d_{i,j}$ is the Euclidean distance between node i and node j. Then, $\mathcal{L}(d_{i,j}) = |d_{i,j}|^{-\alpha}$, where α is the path-loss exponent, with $3 \leqslant \alpha \leqslant 6$.

In addition, according to NEW-LEACH algorithm discussed above, we can increase the value of SINR by clustering sensors into groups. Because in this case, all the sensor nodes will only communicate data with cluster heads, then cluster heads will transmit the aggregated data to the processing center. We define the maximum possible distance R_{max} at which a process point can be the away from its nucleus in a Voronoi cell. Define k to be the number of hops away from the cluster head. Setting $k = R_{max}/R_c$ [4]. Let R_ρ be the radius of the minimal ball centered around the nucleus in the the Voronoi cell, and $P_R = \Pr\{R_\rho > R\}$. Then as it proved in [11], the value of R_{max} is

$$R_{max} = \sqrt{\frac{-0.917\lambda \log\left(\frac{P_R}{7}\right)}{p_1}}. \tag{28}$$

Set P_R to be very small in order to ensure small energy consumption. According to this, the Euclidean distance between node i and node j cannot be larger than R_{max}. That is, $d_{i,j} \leqslant R_{max}$. The path-loss function should satisfy that $\mathcal{L}(d_{i,j}) \geqslant R_{max}^{-\alpha}$. Thus, we have larger received power for incoming signals of interest.

V. Simulation Evaluations

We use MATLAB simulation to evaluate and validate our proposed schemes. The parameters we use in our model are as follows: $R_s = 10m$, $R_f = 0.05m$, $\theta = \pi/6$, $V = 100^3 m^3$, $E_0 = 0.5J$, $\Gamma = 1$, $\alpha = 3$, $P_R = 0.01$ and $B = 100$. Fig. 6 shows the relationship between λ and the probability that $e_{i,j}$ is closed in omnidirectional sensor network. From Fig. 6, we can observe that the critical density is $\lambda_l = 0.00007$ and $\lambda_u = 0.00008$. Because $\lambda = N/\|V\|$, subject to the minimum exposure-path prevention probability constraint, the optimal number of nodes that should be deployed in the entire sensing space is equal to 80 in 3D omnidirectional WCSNs.

To validate the critical deployed density λ_c in our schemes do reduce the total energy consumption, we compare the residual energy with different deployed densities. Fig. 7 shows that as the deployed density λ increases, the average residual energy for each node decreases. It implies that when we apply our critical deployed density in NEW-LEACH, we are able to maximize the residual energy. For mitigation of interference, we observe that there is an $11dB$ gap between the graphs when the interferences are neglected ($\gamma = 0$) or not ($\gamma = 0.01$), as shown in Fig. 8. This implies that we need to consider the impact of the interference. Therefore, all the simulation results above show that our proposed schemes can optimize the tradeoff between power consumption and coverage rate over 3D WCSNs. From Fig 9, we can observe that SINR decreases while λ increases. The difference between each plot reduces gradually when λ increases, which implies when λ

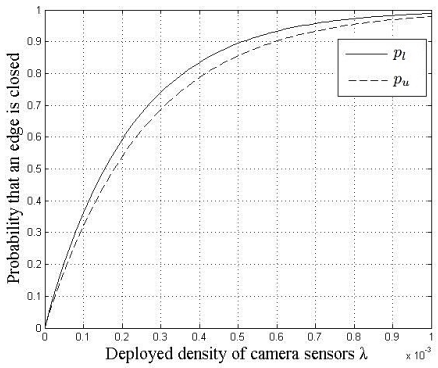

Fig. 6. Relationship between λ and the probability that $e_{i,j}$ is closed in omnidirectional sensor network.

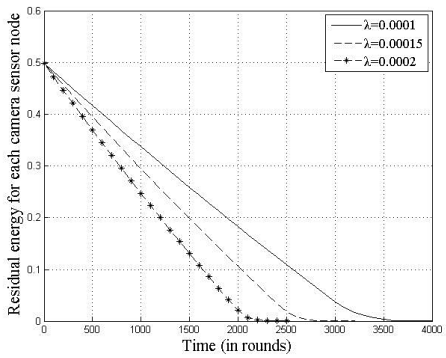

Fig. 7. Average residual energy for each camera sensor node.

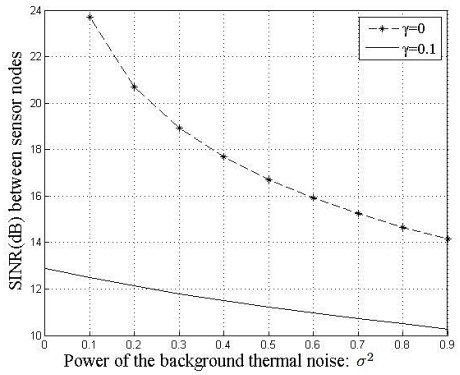

Fig. 8. SINR as a function of σ^2 and γ.

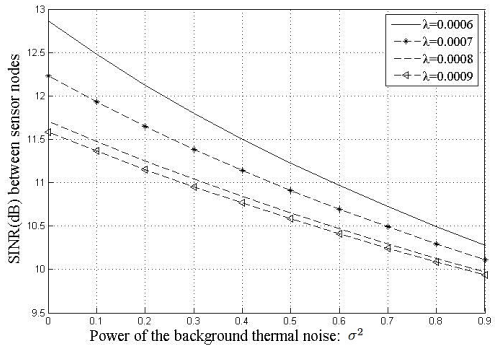

Fig. 9. SINR as a function of σ^2 and γ.

approaches a saturation point asymptotically, SINR finally remains unchanged when λ is above the saturation point. Therefore, we can observe that the critical deployed density λ can reduce the interference among sensor nodes.

VI. Conclusions

We proposed the 3D percolation theory-based exposure-path prevention scheme for optimizing the tradeoff between power consumption and coverage rate over clustered WCSNs. We applied and extended the bond-percolation theory to derive the optimal density of camera sensors deployed using the Poisson distribution in 3D WCSNs subject to the minimum exposure-path prevention probability constraint. We also applied the mutual entropy to analyze the dependency among 3D neighboring camera sensors, justifying the bond-percolation theory in 3D WCSNs. Finally, we applied NEW-LEACH architecture into our 3D WCSNs for power saving and interference mitigation. The conducted extensive simulations show that our proposed schemes outperform the other existing schemes in optimizing the tradeoff between power consumption and coverage rate over 3D WCSNs.

References

[1] L. Liu, X. Zhang, and H. Ma, "Percolation theory-based exposure-path prevention for wireless sensor networks coverage in internet of things," *IEEE Sensor Journal*, vol. 13, no. 10, pp. 3625–3636, 2013.

[2] G. Smaragdakis, I. Matta, and A. Besravros, "Sep: A stable election protocol for clustered heterogeneous wireless sensor networks," in *Boston University Computer Science Department, Tech. Rep.*, 2004.

[3] L. Xie and X. Zhang, "3D clustering-based camera wireless sensor networks for maximizing lifespan with minimum coverage rate constraint," in *IEEE GLOBECOM 2013*, Atlanta, GA, USA, pp. 298–303.

[4] H. Kesten, *Percolation theory for mathematicians*. Boston, MA, USA: Birkhauser, 1982.

[5] G. Grimment, *Percolation, 2nd Ed.* New York, NY, USA: Springer-Verlag, 1999.

[6] J. Wang, Z. Zhou, W. Zhang, T. M. Garoni, and Y. Deng, "Bond and site percolation in three dimensions," in *PHYSICAL REVIEW E 87, 052107*, 2013.

[7] M. Studeny and J. Vejnarova, "The multiinformation function as a tool for measuring stochastic dependence," *Learning in Graphical Models*, vol. 89, pp. 261–297, 1998.

[8] T. V. de Cruys, "Two multivariate generalizations of pointwise mutual information," in *DiSCo 2011, Proceedings of the Workshop on Distributional Semantics and Compositionality*, Stroudsburg, PA, USA, pp. 16–20.

[9] O. Dousse, F. Baccelli, and P. Thiran, "Impact of interferences on connectivity in ad hoc networks," in *IEEE INFOCOM 2003*, pp. 2791–2795.

[10] O. Dousse, M. Franceschetti, N. Macris, R. Meester, and P. Thiran, "Percolation in the signal to interference ratio graph," *Journal of Applied Probability*, vol. 43, no. 2, pp. 552–562, 2006.

[11] S. Bandyopadhyay and E. J. Coyle, "An energy efficient hierarchical clustering algorithm for wireless sensor networks," in *INFOCOM 2003. Twenty-Second Annual Joint Conference of the IEEE Computer and Communications. IEEE Societies*, vol. 3, 2003, pp. 1713–1723.